# DEM Based Overland Flow Routing Model

By Menghua Wang[1] and Allen T. Hjelmfelt[2]

**Abstract:** A physically based, distributed rainfall-runoff event model is developed to route overland flows from flat agricultural watersheds. The model works on a cell basis and routes overland flows from one cell to the next following the maximum downslope directions. The model is able to consider spatially-varied data of soils, crops, land slopes, and aspects, which can be extracted from geographic information systems (GIS) and from digital elevation models (DEMs). Because of this feature, the model can be used for evaluating the impacts of agricultural practices on surface runoff. To describe overland flows on flat watersheds, the model uses the diffusion wave approximation of the St. Venant equations for computing the hydrograph. The computation is accomplished using the MacCormack scheme, a second order accurate numerical method. The model was tested against analytic solutions of the kinematic wave equations and was applied to route the overland flows across Goodwater Creek, a USDA research watershed. The model was calibrated using 26 events and verified using 11 events. The results show that the model works well.

## INTRODUCTION

A physically based, distributed rainfall-runoff model, developed to route overland flows across a watershed during a single storm event, is described. The model was designed for application to Goodwater Creek, an experimental watershed established by the USDA Agricultural Research Service in 1971, but can be used in other watersheds because it is physically based. The Goodwater Creek watershed is located in Central Missouri in the Central Claypan major land resource area. The watershed is on a glacial till plain that has a level to gently sloping surface that is covered with a layer of loess. This layer of loess contains a claypan located 15–30 cm below the surface. The objectives for which the experimental watershed was established were the following: (1) To determine the influence of precipitation characteristics and of watershed scale on water yield and flood hydrograph characteristics; and (2) to determine the basic mechanics of the runoff and interflow process. In 1990 water quality investigations were added as important objectives. The basic mechanics of interflow in these claypan soils was investigated experimentally by Minshall and Jamison (1965), Jamison and Peters (1967), and theoretically by Pi and Hjelmfelt (1994). Based upon the experimental interflow investigations and other preliminary studies, the hydrologic characteristics of the claypan watershed were expressed as: (1) Negligible amounts of precipitation are contributed to ground water; (2) negligible loss of streamflow from the channel to the valley alluvium; (3) negligible amounts of carry-over effect of streamflow from one year to another; and (4) surface runoff supplies the only significant contribution to streamflow. We have found these soils and hydrologic characteristics to describe the Goodwater Creek watershed.

Several runoff simulation models have been applied to the Goodwater Creek watershed in an attempt to generalize the hydrologic observations. This model work began two decades ago with application of USDAHL-70 (Holtan and Lopez 1971). Success was limited (L. Kramer personal communication 1978). Other models have been applied in the intervening years, also with limited success. For a discussion of a recent application of SWAT (Arnold et al. 1994) see Heidenreich (1996). Experience with the readily available models led us to construct a model with the soil and hydrologic characteristics of our watershed in mind at the formulation stage. In addition, our model was designed around a geographic information system (GIS) and digital elevation models (DEMs), so that the influence of spatial variation of hydrologic parameters and of agricultural management systems can be evaluated.

In our distributed-parameter model, the watershed is subdivided into cells. Spatial variability is allowed from one cell to the next; each cell, however, is represented as a homogeneous unit. A DEM is a numerical representation of landscape topography. DEMs for our watershed, available from the U.S. Geological Survey, give elevations with one meter resolution on a rectangular grid with dimensions of 30 m × 30 m. This rectangular grid forms the basis for the cell pattern used by the model. Geometric properties of the watershed, such as flow links and land slopes, used in the model are determined from a DEM as described by Wang (1995). The one meter resolution of the DEM can add artificial topography to our watershed in the form of depressions. Nearly 60% of the cells in the DEM have no outflow direction; that is, they are depression or flat areas.

Overland flow is described using the diffusion wave model due to the very flat slopes on our watershed. Gonwa and Kavvas (1986) have demonstrated that the diffusion wave approximation to full St. Venant equations is appropriate for many cases of practical interest. Two-dimensional diffusion wave runoff models were described by Saghafian et al. (1995), Ogden et al. (1995), and Julien et al. (1995). They applied their models to a steeply sloping basin located in southwestern Idaho. In our case, the one meter resolution of our DEM and the flat topography of our watershed led us to use a one-dimensional formulation of the diffusion wave equation. In our model, the numerical solution to the diffusion wave approximation was accomplished through the MacCormack (1969) method. Infiltration is estimated using the Green and Ampt (1911) approach adapted for layered soils. Due to the flat slopes and the claypan, saturation of the topsoil layer is a primary mechanism for runoff production. This saturation occurs first on the ridges and progresses down slope toward the drainage ways.

The objective of this paper is to develop a physically based, distributed rainfall-runoff model which has the abilities to: (1) accurately simulate overland flows from flat watersheds during single storm events; (2) consider spatially varied soils, crops, and other hydrologic characteristics, so that the model can be used for evaluating the impacts of agricultural practices on surface runoff; and (3) include nonpoint pollutant components for water quality study. The model is tested against analytical

[1]Res. Assoc. Biol. and Agric. Engrg. Dept., Univ. of Missouri, Columbia, MO 65211.

[2]Res. Hydr. Engr., USDA-Agric. Res. Service, Cropping Sys. and Water Quality Res. Unit, Columbia, MO.

Note. Discussion open until June 1, 1998. To extend the closing date one month, a written request must be filed with the ASCE Manager of Journals. The manuscript for this paper was submitted for review and possible publication on November 21, 1995. This paper is part of the ***Journal of Hydrologic Engineering***, Vol. 3, No. 1, January, 1998. ©ASCE, ISSN 1084-0699/98/0001-0001–0008/$4.00 + $.50 per page. Paper No. 12077.

solutions of the kinematic wave equation and is applied to Goodwater Creek, a flat USDA agricultural watershed in a claypan soil region.

## DIFFUSION WAVE MODEL

The model is organized on a cell basis. Each cell has eight possible flow directions, as shown in Fig. 1. Within a cell overland flow is routed along one flow direction. The flow direction is the maximum downslope direction which is determined from the DEM. The routing equations are the continuity equation

$$\frac{\partial h}{\partial t} + \frac{\partial (uh)}{\partial x} = r - f \tag{1}$$

the diffusion wave equation

$$S_f = S_0 - \frac{\partial h}{\partial x} \tag{2}$$

and Manning's equation

$$u = \frac{\zeta}{n} R^{2/3} \sqrt{S_f} \tag{3}$$

where $t$ = time coordinate; T; $h$ = depth of flow, L; $x$ = distance in flow direction, L; $u$ = depth average flow velocity, L/T; $r$ = net rainfall intensity, L/T; $f$ = infiltration rate, L/T; $S_0$ = bed slope in flow direction; $S_f$ = friction slope in flow direction; $\zeta$ = 1 for SI units and 1.49 for imperial units; $R$ = hydraulic radius; and $n$ = Manning's roughness. For overland flow, the hydraulic radius ($R$) is assumed to equal the depth of flow ($h$). In this case, Manning's equation is expressed

$$u = \frac{\xi}{n} h^{2/3} \sqrt{S_f} \tag{4}$$

Manning's $n$ depends on the condition of soil surface and the vegetative cover and serves as a correction factor for the hydraulic radius approximation.

The numerical solution is achieved using a finite difference formulation based on the DEM grid. Thus, the continuity equation for a cell can be written as

$$\frac{\partial h}{\partial t} = \frac{1}{\delta^2} (Q_{\text{in}} - Q_{\text{out}}) \tag{5}$$

where

$$Q_{\text{in}} = Q_{\text{up}} + \delta^2 (r - f) \tag{6}$$

and $\delta$ = cell width, L; $Q_{\text{in}}$ = total inflow, $L^3/T$; $Q_{\text{up}}$ = inflow from adjacent upstream cells, $L^3/T$; and $Q_{\text{out}}$ = outflow, $L^3/T$.

An explicit numerical approximation method based on the MacCormack (1969) scheme is used for solving the routing

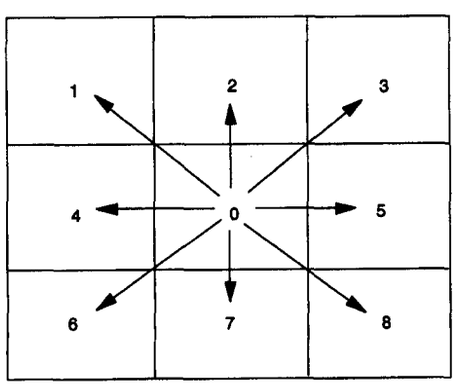


**FIG. 1. Eight Possible Flow Directions of a Cell**

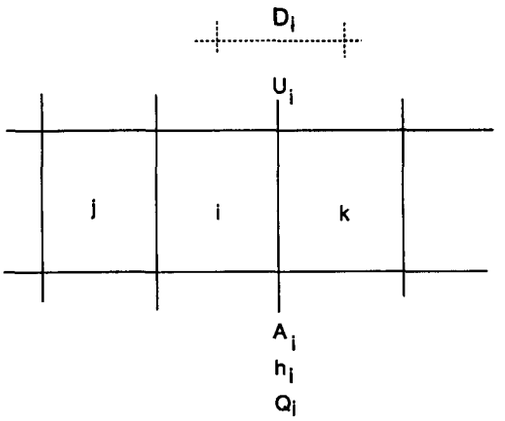


**FIG. 2. One-Dimensional Finite Difference Computation**

equations. This technique is a second order accurate, two-step finite-difference predictor-corrector method. For the spatial derivatives, forward finite-differences are used in the predictor portion and backward finite-differences are used in the corrector portion. For a general one-dimensional computation, as shown in Fig. 2, the finite difference equations are:

Predictor

$$Q^m_{\text{up}_i} = \sum Q^m_{\text{out}_j}; \quad Q^m_{\text{in}_i} = Q^m_{\text{up}_i} + \delta^2 (r_i^{m+1/2} - f_i^{m+1/2}) \tag{7, 8}$$

$$h_i^* = h_i^m + \frac{\Delta t}{\delta^2} (Q^m_{\text{in}_i} - Q^m_{\text{out}_i}) \tag{9}$$

Corrector

$$S^*_{f_i} = S_{0_i} - \frac{h_k^* - h_i^*}{D_i}; \quad U_i^* = \frac{\zeta}{n} \left( \frac{h_i^* + h_k^*}{2} \right)^{2/3} \sqrt{S^*_{f_i}} \tag{10, 11}$$

$$Q^*_{\text{out}_i} = U_i^* A_i^* = U_i^* \delta \frac{h_i^* + h_k^*}{2}; \quad Q^{m+1/2}_{\text{out}_i} = \frac{1}{2} (Q^m_{\text{out}_i} + Q^*_{out_i}) \tag{12, 13}$$

$$Q^{m+1/2}_{\text{in}_i} = \sum Q^{m+1/2}_{\text{out}_j} + \delta^2 (r_i^{m+1/2} - f_i^{m+1/2}) \tag{14}$$

$$h^{**} = h_i^m + \frac{\Delta t}{\delta^2} (Q^{m+1/2}_{\text{in}_i} - Q^{m+1/2}_{\text{out}_i}) \tag{15}$$

and

$$h_i^{m+1} = \frac{1}{2} (h_i^* + h_i^{**}); \quad S^{m+1}_{f_i} = S_{0_i} - \frac{h_k^{m+1} - h_i^{m+1}}{D_i} \tag{16, 17}$$

$$U_i^{m+1} = \frac{\zeta}{n} \left( \frac{h_i^{m+1} + h_k^{m+1}}{2} \right)^{2/3} \sqrt{S^{m+1}_{f_i}} \tag{18}$$

$$Q^{m+1}_{\text{out}_i} = U_i^{m+1} A_i^{m+1} = U_i^{m+1} \delta \frac{h_i^{m+1} + h_k^{m+1}}{2} \tag{19}$$

where $m$ = time step; $\Delta t$ = time interval, T; $D$ = distance between the cell centers of $I$ and $k$, L; $j$ = upstream cell number; and $k$ = downstream cell number.

The equations defined from (7)–(19) can be directly applied to cells with water flowing to the cell directly above, directly below, to the right, or to the left (i.e., not pointing to corner cells). In this case, the flow routing distance ($D$) is equal to $\delta$. The flow directions are determined from the DEM.

For a cell with a flow direction pointing to a corner cell, as shown in Fig. 3, overland flow is routed along the diagonal line. In this case the flow routing distance ($D$) is equal to $\delta\sqrt{2}$, and the outflow rate ($Q_{\text{out}}$) is computed using the following equations

$$Q_{\text{out}_i} = \delta \left( U_{i,t} \frac{h_i + h_t}{2} + U_{i,o} \frac{h_i + h_o}{2} \right) \tag{20}$$

where

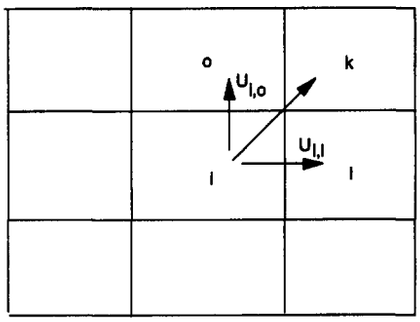


**FIG. 3. Computational Analog for a Cell with Flow Direction Pointing to a Corner Cell**

$$U_{i,l} = U_{i,o} = \frac{\sqrt{2}}{2} U_i \tag{21}$$

Substituting (21) into (20) leads to

$$Q_{\text{out}_i} = \frac{\sqrt{2}}{2} \delta U_i \frac{2h_i + h_o + h_l}{2} \tag{22}$$

If the flow depths in the cells of $k$, $l$, and $o$ are assumed equal, (22) becomes

$$Q_{\text{out}_i} = \sqrt{2} U_i \delta \frac{h_i + h_k}{2} \tag{23}$$

The MacCormack scheme is stable if the Courant-Friedrichs-Lewy (CFL) criterion is satisfied. The CFL criterion can be expressed as (Weinmann and Laurenson 1979; Huang and Song 1985; Gharangik and Chaudhry 1991)

$$\frac{\Delta t}{\delta} \leq \frac{1}{u + \sqrt{gh}} \tag{24}$$

where $g$ = acceleration due to gravity, $L/T^2$.

The initial condition for overland flow is a dry surface

$$h_i^0 = Q_{\text{out}_i}^0 = 0, \; i = 1, 2, \ldots N \tag{25}$$

where $N$ is the total number of cells in a watershed. The boundary condition for the cells on the upstream ends are taken as zero inflow. Thus,

$$Q_{\text{up}} = 0 \tag{26}$$

For the outlet cell at the downstream end, a zero-depth gradient boundary condition is employed (Morris 1979; Govindaraju et al. 1990; Tayfur et al. 1993). The zero-depth gradient condition can be written as

$$h_N = h_{N+1} \tag{27}$$

where $N$ = the outlet cell number.

Overland flows are routed starting from the most upstream cells and ending with the downstream cell, as a cascading system, using the finite difference equations and following the computation sequences determined by DEM.

## INFILTRATION

The Green and Ampt equation is used for infiltration computation. The basic equation is

$$f_c = K_s \frac{Z + S_w}{Z} \tag{28}$$

where $f_c$ = infiltration capacity rate, L/T; $K_S$ = saturated hydraulic conductivity of the wetted zone, L/T; $S_W$ = average suction at the wetting front, L; and $Z$ = depth of the wetting front, L. The infiltration rate for cell $i$ in time step $m + 1$ is computed as

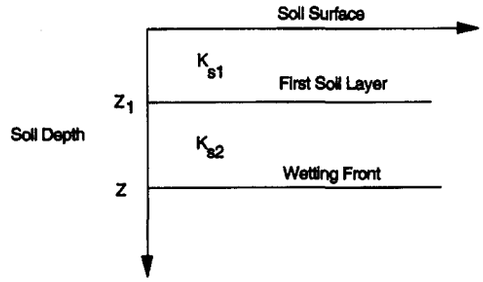


**FIG. 4. Two Layer Soil Profiles with Different Properties**

$$f_i^{m+1/2} = \min\left(f_{c_i}^m, \; r_i^{m+1/2} + \frac{h_i^m}{\Delta t}\right) \tag{29}$$

in which

$$f_{c_i}^m = K_s \frac{Z_i^m + S_{w_i}}{Z_i^m} \tag{30}$$

Eq. (29) indicates that infiltration occurs at the potential rate any time that rainfall plus detention storage can satisfy the demand.

The wetting front depth ($Z^{m+1}$) in the end of time step $m + 1$ is calculated by the recurrence formula

$$Z_i^{m+1} = Z_i^m + \frac{f_i^{m+1/2} \Delta t}{\theta_{s_i} - \theta_i} \tag{31}$$

where $\theta_s$ = effective porosity; and $\theta$ = initial moisture content. If the potential infiltration rate exceeds the rainfall intensity and detention storage is zero, as at the beginning of the first time step when the wetting front depth ($Z$) and the overland flow depth ($h$) are zero, the infiltration rate is equal to the rainfall intensity.

The infiltration equations (29)–(31) are for a uniform soil profile. For a two layer soil profile, as shown in Fig. 4, the infiltration rate is calculated by the same formulas as for a uniform soil profile when the wetting front is in the first layer. When the wetting front is in the second layer, (29)–(31) can still be used. The effective porosity ($\theta_s$) and the initial moisture ($\theta$), however, must be replaced by using the corresponding parameters in the second layer, and the hydraulic conductivity $K_s$ in the wetted zone is calculated by

$$K_s = \frac{Z}{\frac{Z_1}{K_{s1}} + \frac{Z - Z_1}{K_{s2}}} \tag{32}$$

where $Z$ = depth of the wetting front, L; $Z_1$ = depth of the first soil layer, L; $K_{s1}$ = saturated hydraulic conductivity of the first soil layer, L/T; and $K_{s2}$ = saturated hydraulic conductivity of the second soil layer, L/T.

## MODEL APPLICATION

The physically based, distributed model was tested against the analytic solutions of the kinematic wave equation for a simple geometric plane with a steeper slope, where the diffusion term, $\partial h/\partial x$ in our model, can be neglected. The kinematic wave solutions were given by Woolhiser (1975). The plane is assumed to be impermeable, to have a unit width, a length of 30.48 m, and a slope of 0.05, and to receive rainfall at a constant rate of 7.62 cm/h. The results from our model and the analytic solutions of the kinematic wave equation are identical as shown in Fig. 5.

The tested model was applied to route overland flows from Goodwater Creek, a small watershed located in central Missouri. This 12.2 $km^2$ agricultural watershed was established as a research catchment by the U.S. Department of Agriculture,

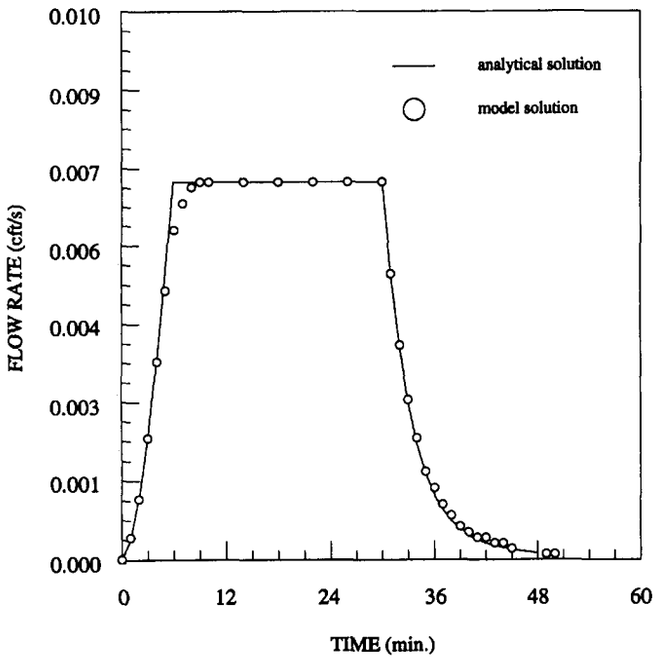


**FIG. 5. Model Testing Using an Analytical Solution for a Simple Watershed Geometry with Constant Rainfall**

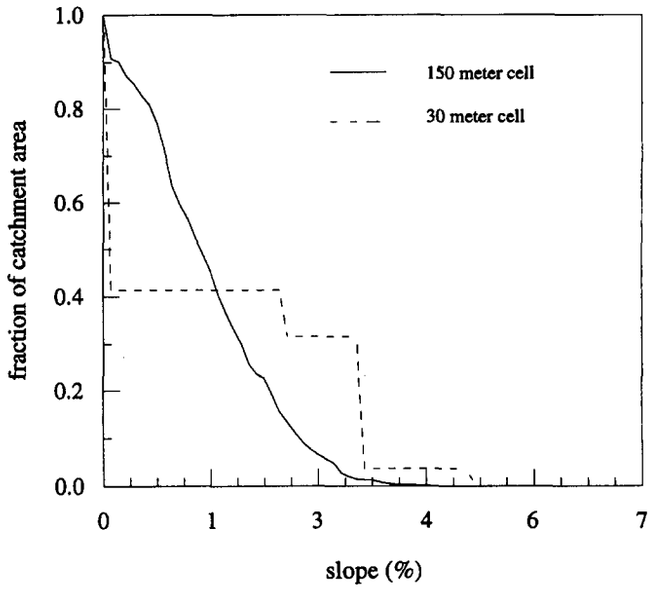


**FIG. 6. Accumulative Frequency Distribution of Catchment Area and Land Slope for Goodwater Creek Watershed**

Agricultural Research Service in 1971. On the study watershed, rainfall is measured using a weighing rain gauge. Runoff is measured using a triangular weir which provides control for low flows. The channel and a bridge opening provide control for higher flows. Thirty-seven of the largest observed rainfall-runoff events were selected from seventeen years of measurements for analysis. The topographic information for the watershed is available from the U.S. Geological Survey in the form of a digital elevation model. The horizontal and vertical resolutions of the DEM are 30 m and 1 m, respectively. This results in 13,556 cells in the watershed. Computations using all 13,566 cells is time consuming. To create a more usable representation of the watershed, Wang (1995) aggregated the original DEM cells into larger cells. The cell size for the model application is 150 m × 150 m. Each 150 m × 150 m grid contains 25 original cells. The aggregation algorithm treats the grid of original cells to be aggregated as a small watershed. The flow direction of the grid is determined based on the flow path that the small watershed outlet would take. After this aggregation, the number of cells is reduced from 13,556 to 543. The land slope of a grid is calculated by averaging the slope values of the 25 original cells within the grid. The distributions of land slopes for the original DEM cells and the aggregated cells are given in Fig. 6. The vertical resolution of 1 m for the DEM causes almost 60% of the original cells of this watershed to have zero for the computed land slope values. After DEM aggregation, the accumulative frequency distribution curve of catchment areas with land slopes becomes more smooth. The data accuracy for a DEM with 1 m of vertical resolution is 0.5 m. The corresponding data accuracy for land slope calculation is 0.5 m divided by the cell size of 30 m, or about 1.6%. Fig. 6 shows that the differences of land slopes between the aggregated grids and the original DEM cells are within the data accuracy of land slopes. The land slope average method for DEM aggregation slightly increases the computed slope values in flat areas and decreases the slope values in steep areas.

Infiltration computation requires estimates of hydraulic conductivity ($K_s$), effective porosity ($\theta_s$), and the relationship between wetting front capillary pressure head ($S_w$) and initial soil moisture ($\theta$). The hydraulic conductivity, effective porosity, and capillary pressure head were determined based on an unpublished report (Jamison et al. 1964). The generalized properties of the soil profile of Goodwater Creek watershed are listed in Table 1. The top two soil layers are Mexico silt loam. The soil hydraulic properties for these upper two layers are within the range of those given by Brakensiek and Rawls (1982) for silt loam and silty clay loam soils. The third layer is clay, which is assumed to be impermeable. Infiltration will stop when the wetting front reaches the clay layer. The hydraulic conductivity for this layer is an order of magnitude less than that listed by Brakensiek and Rawls (1982) for clay. The moisture characteristics, measured by Jamison, for the upper two layers are shown in Fig. 7. This figure was used to determine the suction head for a given initial moisture.

Initial soil moisture and Manning's roughness coefficient ($n$) are treated as model parameters. Initial soil moisture is associated with infiltration, so this parameter controls the volume of total runoff. The Manning's roughness coefficient depends on land surface so this is the parameter that controls fitting to runoff hydrograph and its peak discharge. In this study, 26 of the 37 rainfall-runoff events were used for the parameter calibration. The goodness of fit for the total hydrograph is described by the root-mean-square error. The ability to predict the peak discharge is expressed by the percent error.

The initial soil moisture was assumed to be uniform and was calibrated to make the computed runoff volume for each event match the measured volume. The calibrated initial moisture for most of the 26 events was near saturation. Analysis of rainfall that occurred prior to each of the events showed that this was consistent with actual watershed conditions. The claypan soil on flat slopes regularly results in saturation of the

**TABLE 1. Soil Properties of Land Profile in Goodwater Creek Watershed**

| Soil depth (cm) (1) | Soil texture (2) | Porosity (3) | Hydraulic conductivity (cm/h) (4) |
|---|---|---|---|
| 0–25 | Silt loam | 0.486 | 0.292 |
| 25–33 | Silt loam | 0.510 | 0.417 |
| 33–45 | Clay | — | 0.008 |

Note: From an unpublished report (Jamison et al. 1964).

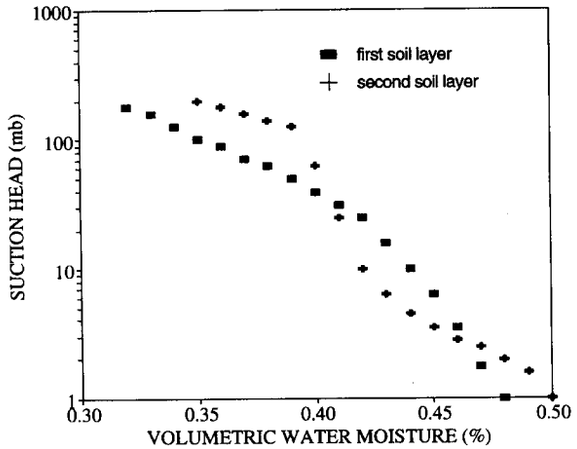


**FIG. 7. Measured Moisture Characteristics for Two Layer Soil Profiles of Goodwater Creek (from an unpublished report by Jamison et al. 1964)**

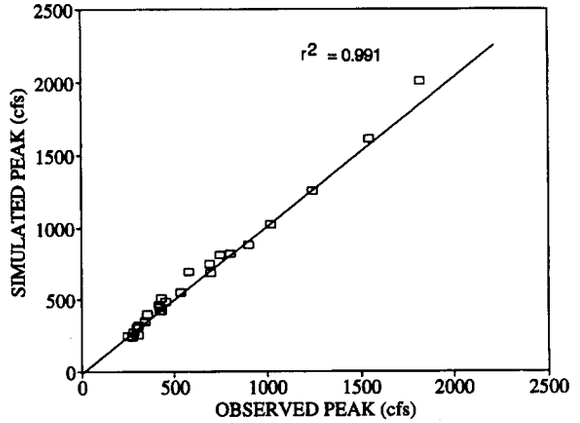


**FIG. 8. Comparison of Observed and Simulated Peak Discharges Using Individual Manning's *n* for 26 Storm Events**

topsoil layer. Water is often visible in depression storage for several days during a wet period.

Manning's $n$ for channel cells is assumed to be 0.1. The channel cell is defined as a cell with flow convergence. The channel cells were determined using a catchment area threshold value from DEMs (Wang 1995). In this small watershed the main drainage way is little more than a swale or a grassed waterway for much of its length. We routed the flow through the drainage way as overland flow. This approximation was also used by Saghafian et al. (1995) and Ogden et al. (1995). The Manning's roughness coefficients for all of the overland flow cells within a watershed were assumed to be the same and were calibrated for each storm event. The calibrated Manning's roughness coefficient ($n$) and the simulated result for each of the 26 storm events are listed in Table 2. Fig. 8 is a scatter plot of observed versus simulated peak discharges. The $R$-square value is 0.991. The peak discharge errors range from 0.02% to 19.73%, with a mean value of 6.11. The average root-mean-square error for fitting the runoff hydrographs is 93.64. The average Manning's $n$ for the 26 storm events was 0.246, and it varied between 0.12 and 0.40. These values are comparable to those listed by Engman (1986) and Huggins et al. (1975, referred to by Engman). Table 2 shows that large storm events have large values of Manning's $n$ and small events have small Manning's $n$. This is consistent with the relation for Manning's coefficient, $n$, against flow depth given by Ree and Palmer (1949, referred to by Barling and Moore 1994). Flows at very shallow depths encounter maximum resistance because the vegetation is upright in the flow (Barling and Moore 1994). In the case of overland flow, Manning's roughness ($n$) not only depends on the condition of soil surface and the vegetative cover, but serves as a correction factor for the hydraulic radius approximation.

Table 3 and Fig. 9 give the simulation results for the 26

**TABLE 2. Comparison of Observed and Computed Peak Discharges and Runoff Hydrographs Using Calibrated Manning's *n* for 26 Storm Events**

| | | | Peak Discharge | | | Hydrograph |
|---|---|---|---|---|---|---|
| Flood (1) | Flood date (2) | $n$ (3) | Observed ($m^3/s$) (4) | Computed ($m^3/s$) (5) | Error (%) (6) | Error (RMS)[a] (7) |
| 1 | May 6, 1977 | 0.12 | 7.79 | 6.76 | 13.22 | 45.97 |
| 2 | May 30, 1974 | 0.25 | 21.18 | 22.86 | 7.92 | 99.93 |
| 3 | September 23, 1986 | 0.20 | 8.57 | 8.98 | 4.72 | 50.52 |
| 4 | July 3, 1980 | 0.23 | 11.73 | 13.08 | 11.54 | 55.97 |
| 5 | May 16, 1986 | 0.12 | 8.72 | 7.21 | 17.33 | 60.94 |
| 6 | April 30, 1983 | 0.18 | 19.81 | 19.28 | 2.69 | 89.90 |
| 7 | March 3, 1976 | 0.14 | 7.03 | 6.99 | 0.56 | 41.18 |
| 8 | June 8, 1974 | 0.21 | 8.42 | 8.45 | 0.39 | 56.97 |
| 9 | June 19, 1983 | 0.14 | 9.64 | 9.94 | 3.10 | 80.67 |
| 10 | July 24, 1981 | 0.14 | 7.92 | 7.69 | 2.81 | 50.31 |
| 11 | July 23, 1981 | 0.31 | 35.25 | 35.50 | 0.70 | 148.33 |
| 12 | November 19, 1985 | 0.19 | 15.15 | 15.52 | 2.45 | 95.67 |
| 13 | September 1, 1982 | 0.40 | 43.89 | 45.42 | 3.49 | 248.64 |
| 14 | December 2, 1982 | 0.34 | 28.86 | 28.86 | 0.02 | 111.84 |
| 15 | April 10, 1979 | 0.22 | 12.16 | 11.85 | 2.59 | 81.95 |
| 16 | June 19, 1981 | 0.40 | 51.48 | 56.82 | 10.37 | 172.66 |
| 17 | June 16, 1985 | 0.37 | 25.39 | 24.95 | 1.73 | 153.50 |
| 18 | October 3, 1984 | 0.30 | 22.71 | 23.01 | 1.31 | 140.04 |
| 19 | November 18, 1985 | 0.31 | 16.33 | 19.49 | 19.34 | 87.49 |
| 20 | August 1, 1978 | 0.29 | 11.94 | 11.99 | 0.40 | 72.15 |
| 21 | June 8, 1984 | 0.36 | 19.57 | 21.00 | 7.32 | 147.59 |
| 22 | August 29, 1982 | 0.15 | 9.67 | 9.60 | 0.78 | 83.90 |
| 23 | June 8, 1982 | 0.31 | 12.08 | 14.46 | 19.73 | 64.59 |
| 24 | August 26, 1982 | 0.25 | 12.79 | 13.73 | 7.34 | 63.59 |
| 25 | May 28, 1989 | 0.20 | 10.02 | 11.26 | 12.33 | 45.51 |
| 26 | July 30, 1989 | 0.27 | 11.90 | 12.45 | 4.54 | 84.73 |
| [Average values] | | 0.246 | — | — | 6.11 | 93.64 |

[a]RMS, root mean square.

**TABLE 3. Comparison of Observed and Computed Peak Discharges and Runoff Hydrographs Using Average Manning's *n* for 26 Storm Events**

| | | | Peak Discharge | | | Hydrograph |
|---|---|---|---|---|---|---|
| Flood (1) | Flood date (2) | $n$ (3) | Observed ($m^3/s$) (4) | Computed ($m^3/s$) (5) | Error (%) (6) | Error (RMS)[a] (7) |
| 1 | May 6, 1977 | 0.246 | 7.79 | 4.43 | 43.14 | 78.70 |
| 2 | May 30, 1974 | 0.246 | 21.18 | 23.02 | 8.65 | 99.43 |
| 3 | September 23, 1986 | 0.246 | 8.57 | 7.58 | 11.57 | 61.24 |
| 4 | July 3, 1980 | 0.246 | 11.73 | 12.22 | 4.18 | 55.64 |
| 5 | May 16, 1986 | 0.246 | 8.72 | 5.12 | 41.29 | 80.56 |
| 6 | April 30, 1983 | 0.246 | 19.81 | 16.51 | 16.66 | 89.79 |
| 7 | March 3, 1976 | 0.246 | 7.03 | 5.38 | 23.50 | 65.26 |
| 8 | June 8, 1974 | 0.246 | 8.42 | 7.44 | 11.65 | 63.78 |
| 9 | June 19, 1983 | 0.246 | 9.64 | 7.33 | 23.94 | 86.84 |
| 10 | July 24, 1981 | 0.246 | 7.92 | 5.96 | 24.76 | 69.60 |
| 11 | July 23, 1981 | 0.246 | 35.25 | 37.96 | 7.67 | 185.17 |
| 12 | November 19, 1985 | 0.246 | 15.15 | 13.22 | 12.77 | 92.82 |
| 13 | September 1, 1982 | 0.246 | 43.89 | 58.02 | 32.21 | 396.41 |
| 14 | December 2, 1982 | 0.246 | 28.86 | 33.76 | 16.97 | 151.98 |
| 15 | April 10, 1979 | 0.246 | 12.16 | 10.98 | 9.71 | 85.76 |
| 16 | June 19, 1981 | 0.246 | 51.48 | 70.18 | 36.32 | 270.71 |
| 17 | June 16, 1985 | 0.246 | 25.39 | 35.61 | 40.24 | 180.72 |
| 18 | October 3, 1984 | 0.246 | 22.71 | 26.23 | 15.47 | 165.28 |
| 19 | November 18, 1985 | 0.246 | 16.33 | 21.29 | 30.36 | 93.31 |
| 20 | August 1, 1978 | 0.246 | 11.94 | 13.48 | 12.93 | 85.38 |
| 21 | June 8, 1984 | 0.246 | 19.57 | 27.19 | 38.92 | 184.79 |
| 22 | August 29, 1982 | 0.246 | 9.67 | 7.71 | 20.31 | 66.08 |
| 23 | June 8, 1982 | 0.246 | 12.08 | 17.74 | 46.86 | 76.20 |
| 24 | August 26, 1982 | 0.246 | 12.79 | 13.77 | 7.64 | 64.01 |
| 25 | May 28, 1989 | 0.246 | 10.02 | 9.38 | 6.41 | 54.05 |
| 26 | July 30, 1989 | 0.246 | 11.90 | 14.15 | 18.88 | 84.05 |
| [Average values] | | 0.246 | — | — | 21.65 | 114.91 |

[a]RMS, root mean square.

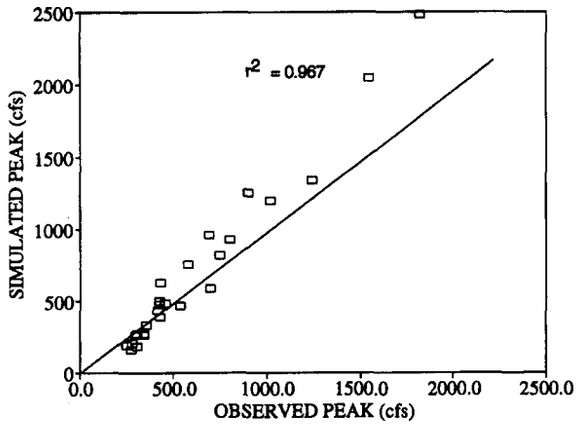


**FIG. 9. Comparison of Observed and Simulated Peak Discharges Using Average Manning's *n* for 26 Storm Events**

rainfall-runoff events using the average Manning's $n$. The $R$-square value between the simulated and observed peak discharges is 0.967. The peak discharge errors range from 4.18% to 46.86%, with a mean value of 21.65. The average root-mean-square error for the runoff hydrographs is 114.91. Comparisons of the runoff hydrographs for two typical storm events are displayed in Figs. 10 and 11. The general shapes of the computed hydrographs are quite good. The average

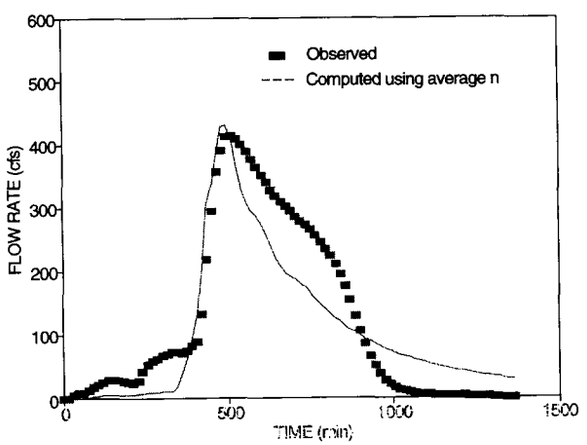


**FIG. 10. Comparison of Observed and Simulated Runoff Hydrograph Using Average Manning's *n* for the Event of July 3, 1980**

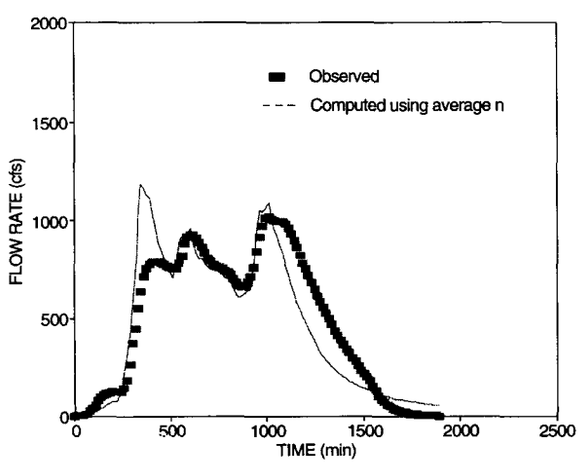


**FIG. 11. Comparison of Observed and Simulated Runoff Hydrograph Using Average Manning's *n* for the Event of December 2, 1982**

**TABLE 4. Comparison of Observed and Computed Peak Discharges and Runoff Hydrographs Using 11 Storm Events for Model Verification**

| | | | Peak Discharge | | | Hydrograph |
|---|---|---|---|---|---|---|
| Flood (1) | Flood date (2) | $n$ (3) | Observed ($m^3/s$) (4) | Computed ($m^3/s$) (5) | Error (%) (6) | Error (RMS)[a] (7) |
| 1 | March 14, 1990 | 0.246 | 28.59 | 26.80 | 6.24 | 80.22 |
| 2 | May 15, 1990 | 0.246 | 20.69 | 22.05 | 6.53 | 77.99 |
| 3 | June 7, 1990 | 0.246 | 13.03 | 11.81 | 9.32 | 77.06 |
| 4 | July 10, 1991 | 0.246 | 13.79 | 14.77 | 7.10 | 94.59 |
| 5 | December 14, 1992 | 0.246 | 10.25 | 8.45 | 17.59 | 42.64 |
| 6 | April 19, 1993 | 0.246 | 10.66 | 10.00 | 6.18 | 66.55 |
| 7 | April 24, 1993 | 0.246 | 6.12 | 3.64 | 40.44 | 41.12 |
| 8 | June 6, 1993 | 0.246 | 7.67 | 5.75 | 25.02 | 46.59 |
| 9 | July 7, 1993 | 0.246 | 9.40 | 8.57 | 8.79 | 77.08 |
| 10 | September 19, 1993 | 0.246 | 6.60 | 5.46 | 17.31 | 26.25 |
| 11 | November 14, 1993 | 0.246 | 7.63 | 7.09 | 7.04 | 65.44 |
| [Average values] | | 0.246 | — | — | 13.78 | 63.23 |

[a]RMS, root mean square.

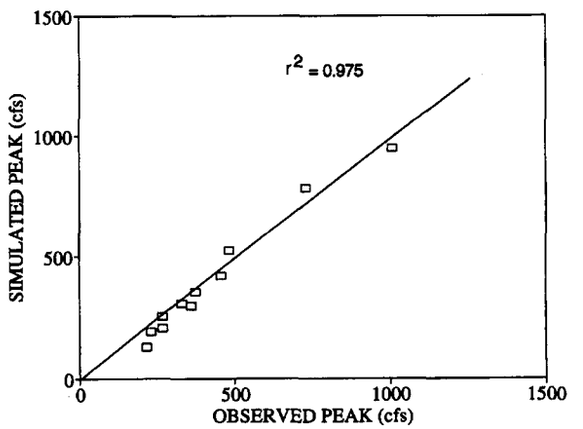


**FIG. 12. Comparison of Observed and Simulated Runoff Hydrograph Using Storm Events for Model Verification**

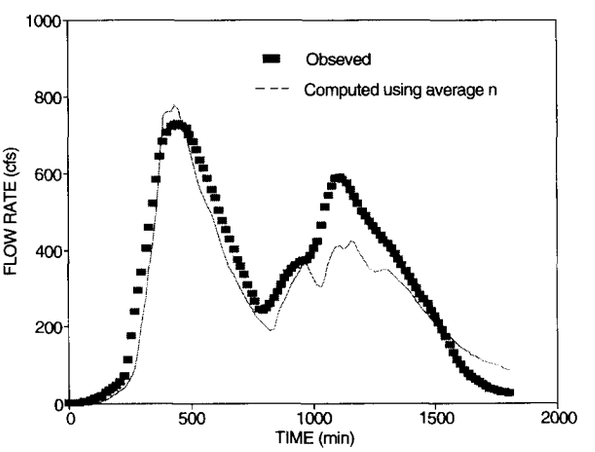


**FIG. 13. Comparison of Observed and Simulated Runoff Hydrograph Using the Event of May 15, 1993 for Model Verification**

Manning's $n$, however, resulted in the computed runoff peak discharges over-estimated for large storm events and under-estimated for small storm events.

The remaining 11 storm events were used for verifying the ability of the model to predict peak discharges and hydrographs using the average Manning's $n$. The initial soil moisture for most of the 11 events was near saturation. The simulated peak discharges and fitting errors are listed in Table 4 and shown in Fig. 12. The average error for peak discharge simulation is 13.78%. The $R$-square error between the simu-

lated and observed peak discharges is 0.975. A comparison of the simulated and observed hydrograph for the verification event of May 15, 1993 is shown in Fig. 13. The verification indicates that the model using the average Manning's $n$ gives very good results. Some runoff peak discharges of the eleven storm events are slightly under-estimated using the average Manning's $n$. The reason is that those events are relatively small events compared with most of the 26 events which were used for the model calibration.

## SUMMARY AND CONCLUSION

A physically based, distributed overland flow routing model was developed to model runoff from storm events on small, flat watersheds. The model works on a cell basis for considering spatially varied soils, crops, and other hydrologic characteristics. The model can be used for evaluating the impacts of agricultural practices on surface runoff and be adapted with nonpoint pollutant components for water quality study.

The model was tested against the analytic solutions of the kinematic wave equation. The results from our model and the analytic solution of the kinematic wave equation for a simple geometric plane with a steeper slope are identical.

Goodwater Creek watershed located in north central Missouri has a level to gently sloping surface covered by a thin top soil layer underlain by a claypan. The spatial variability of surface topography was considered with the aid of DEM analysis. Nearly 60% of the cells needed special consideration because they indicated depressions or flat areas. Infiltration into the topsoil layer was estimated using the Green and Ampt equation. Parameters were determined using results of a previous soil properties investigation. Those properties are close to the properties tabulated by Brakensiek and Rawls (1982) for use with a Green and Ampt based runoff estimation procedure. Runoff was primarily due to saturation of the topsoil layer, which was often nearly saturated at the start of the storms, so that infiltration primarily influenced time to initiation of runoff.

The model was calibrated using 26 events observed on the watershed. The average Manning's roughness ($n$) was 0.246, and varied between 0.12 and 0.40 for the 26 storm events used for model calibration. These values are within the range of values reported by Engman (1986). The average Manning's $n$ of 0.246 was used with the 26 storm events from which the model was calibrated and with the other 11 events for model verification. The verification showed that using the average Manning's $n$ resulted in the computed runoff peak discharges over-estimated in large storm peak discharges and under-estimated in small storm peak discharges. Thus large storm events have larger values of Manning's $n$ whereas small events have smaller Manning's $n$. The average error for peak discharge simulated for the verification events was 13.78%.

## APPENDIX I. REFERENCES


Arnold, J. G., Williams, J. R., Srinivasan, R., King, K. W., and Griggs, R. H. (1994). *SWAT Soil and Water Assessment Tool*, USDA Agricultural Research Service, Temple, Tex.

Barling, R. D., and Moore, I. D. (1994). "Role of buffer strips in management of waterway pollution: a review." *Envir. Mgmt.*, (18)4, 543–558.

Brakensiek, D. L., and Rawls, W. J. (1982). "An infiltration based runoff model for a standardized 24-hour rainfall." *Trans. Am. Soc. Agr. Engrs.*, 25(6), 1607–1611.

Engman, E. T. (1986). "Roughness coefficients for routing surface runoff." *J. Irrig. and Drain Engrg.*, ASCE, 112(1), 39–53.

Gharangik, A. M., and Chaudhry, M. H. (1991). "Numerical simulation of hydraulic jump." *J. Hydr. Engrg.*, 117(9), 1195–1332.

Gonwa, W. S., and Kavvas, M. L. (1986). "A modified diffusion wave equation for flood propagation in trapezoidal channels." *J. Hydro.*, 83, 119–136.

Govindaraju, R. S., Kavvas, M. L., and Jones, S. E. (1990). "Approximate analytical solutions for overland flows." Am. Geophys. Union, *Water Resour. Res.*, 26(12), 2903–2912.

Green, W. H., and Ampt, G. A. (1911). "Studies on soil physics. I: The flow of air and water in soils." *J. Agric. Sci.*, 4, 1–24.

Heidenreich, L. K. (1996). "Economic and water quality assessment of alternative cropping systems in Goodwater Creek watershed, Missouri," MS thesis, Agricultural Economics, University of Missouri at Columbia, Mo.

Holtan, H. N., and Lopez, N. C. (1971). "USDAHL-70 model of watershed hydrology." Tech. Bull. No. 1435, USDA Agricultural Research Service, Beltsville, Md.

Huang, J., and Song, C. C. S. (1985). "Stability of dynamic flood routing schemes." *J. Hydr. Engrg.*, ASCE, 111(12), 1497–1506.

Huggins, L. F., Podmore, T. H., and Hood, C. F. (1975). "Hydrologic simulations using distributed parameters." Purdue University Water Resources Center, West Lafayette, Ind.

Jamison, V. C., Peters, D. L., and Saxton, K. E. (1964). "Subsurface soil moisture flow above the claypan of Mexico silt loam." Unpublished Report, Work Unit/Project No: SWC W3-Cmo-2. USDA, Watershed Research Unit, Columbia, Mo.

Jamison, V. C., and Peters, D. B. (1967). "Slope length of claypan soils affects runoff." Am. Geophys. Union, *Water Resour. Res.*, 3(2), 471–480.

Julien, P. Y., Saghafian, B., and Ogden, F. L. (1995). "Raster-based hydrologic modeling of spatially-varied surface runoff." *Water Resour. Bull.*, 31(6), 523–536.

MacCormack, R. W. (1969). *The effect of viscosity in hypervelocity impact cratering*. Am. Inst. Aeronaut. and Astronaut., N.Y., 69–354.

Minshall, N. E., and Jamison, V. C. (1965). "Interflow in claypan soils." Am. Geophys. Union, *Water Resour. Res.*, 1(3), 381–390.

Morris, E. M. (1979). "The effect of the small-slope approximation and lower boundary conditions on solutions of the Saint-Venant equations." *J. Hydro.*, 40, 31–47.

Ogden, F. L., Richardson, J. R., and Julien, P. Y. (1995). "Similarity in catchment response, 2. Moving rainstorms." Am. Geophys. Union, *Water Resour. Res.*, 31(6), 1543–1547.

Pi, Z., and Hjelmfelt, A. T. (1994). "Hybrid finite analytic solution for lateral subsurface flow." Am. Geophys. Union, *Water Resour. Res.*, 30(5), 1471–1478.

Ree, W. O., and Palmer, V. J. (1949). "Flow of water in channels protected by vegetative linings." *Tech. Bull. 967*, United States Department of Agriculture, Washington, D.C.

Saghafian, B., Julien, P. Y., and Ogden, F. L. (1995). "Similarity in catchment response, 1. Stationary rainstorms." Am. Geophys. Union, *Water Resour. Res.*, 31(6), 1533–1542.

Tayfur, G., Kavvas, M. L., Govindaraju, R. S., and Storm, D. E. (1993). "Applicability of St. Venant equations for two-dimensional overland flows over rough infiltrating surfaces." *J. Hydr. Engrg.*, ASCE, 119(1), 51–63.

Wang, M. (1995). "A dynamic hydrologic and non-point pollutant transport model based on DEMs," PhD thesis, University of Missouri at Columbia, Mo.

Weinmann, P. E., and Laurenson, E. M. (1979). "Approximate flood routing methods: A review." *J. Hydr. Engrg.*, ASCE, 105(12), 1521–1537.

Woolhiser, D. A. (1975). "Simulation of unsteady overland flow." *Unsteady flow in open channels*, K. Mahmood and V. Yevjevich, eds., Vol. II, Water Resources Publications, Fort Collins, Colorado, 485–508.


## APPENDIX II. NOTATION

*The following symbols are used in this paper:*

$A$ = flow cross section area, $L^2$;
$D$ = distance between the cell centers of $I$ and $k$, L;
$f$ = infiltration rate, L/T;
$f_c$ = infiltration capacity rate, L/T;
$g$ = acceleration due to gravity, $L/T^2$;
$h$ = overland flow depth, L;
$I$ = cell number;
$j$ = upstream cell number;
$k$ = downstream cell number;
$K_S$ = saturated hydraulic conductivity of the wetted zone, L/T;
$K_{s1}$ = saturated hydraulic conductivity in the first land layer, L/T;
$K_{s2}$ = saturated hydraulic conductivity in the second land layer, L/T;
$m$ = time step;

$n$ = Manning's roughness coefficient;
$N$ = total number of cells or outlet cell number;
$Q_{in}$ = total inflow, $L^3/T$;
$Q_{out}$ = outflow, $L^3/T$;
$Q_{up}$ = inflow from adjacent upstream cells, $L^3/T$;
$r$ = rainfall intensity, L/T;
$R$ = hydraulic radius, L;
$S_f$ = friction slope in flow direction;
$S_o$ = bed slope in flow direction;
$S_w$ = average suction head at the wetting front, L;
$t$ = time coordinate, T;
$u$ = depth average flow velocity, L/T;
$x$ = distance in flow direction, L;
$Z$ = depth of the wetting front, L;
$Z_1$ = depth of the first soil layer, L;
$\delta$ = element width, L;
$\theta$ = initial moisture content; and
$\theta_s$ = effective porosity.